Author(s): Hulkko, Eero; Pikker, Siim; Tiainen, Ville; Tichauer, Ruth H.; Groenhof, Gerrit; Toppari, Jussi J.

Title: Effect of molecular Stokes shift on polariton dynamics

Year: 2021

Version: Published version

Please cite the original version:

Hulkko, E., Pikker, S., Tiainen, V., Tichauer, R. H., Groenhof, G., & Toppari, J. J. (2021). Effect of molecular Stokes shift on polariton dynamics. Journal of Chemical Physics, 154(15), 154303. https://doi.org/10.1063/5.0037896

Effect of molecular Stokes shift on polariton dynamics

E. Hulkko, S. Pikker, V. Tiainen, R. H. Tichauer, G. Groenhof, and J. J. Toppari

View Online

Export Citation

CrossMark

The Journal of Chemical Physics

AIP Publishing

Effect of molecular Stokes shift on polariton dynamics

E. Hulkko,[1,2] [ID] S. Pikker,[1,3] [ID] V. Tiainen,[1] [ID] R. H. Tichauer,[2] [ID] G. Groenhof,[2] [ID] and J. J. Toppari[1,a)] [ID]

AFFILIATIONS

[1] Department of Physics and Nanoscience Center, University of Jyväskylä, P.O. Box 35, FI-40014 Jyväskylä, Finland
[2] Department of Chemistry and Nanoscience Center, University of Jyväskylä, P.O. Box 35, FI-40014 Jyväskylä, Finland
[3] University of Tartu, Institute of Physics, W. Ostwaldi tn 1, 50411 Tartu, Estonia

Note: This paper is part of the JCP Special Topic on Polariton Chemistry: Molecules in Cavities and Plasmonic Media.
[a)]**Author to whom correspondence should be addressed:** j.jussi.toppari@jyu.fi

ABSTRACT

When the enhanced electromagnetic field of a confined light mode interacts with photoactive molecules, the system can be driven into the regime of strong coupling, where new hybrid light–matter states, polaritons, are formed. Polaritons, manifested by the Rabi split in the dispersion, have shown potential for controlling the chemistry of the coupled molecules. Here, we show by angle-resolved steady-state experiments accompanied by multi-scale molecular dynamics simulations that the molecular Stokes shift plays a significant role in the relaxation of polaritons formed by organic molecules embedded in a polymer matrix within metallic Fabry–Pérot cavities. Our results suggest that in the case of Rhodamine 6G, a dye with a significant Stokes shift, excitation of the upper polariton leads to a rapid localization of the energy into the fluorescing state of one of the molecules, from where the energy scatters into the lower polariton (radiative pumping), which then emits. In contrast, for excitonic J-aggregates with a negligible Stokes shift, the fluorescing state does not provide an efficient relaxation gateway. Instead, the relaxation is mediated by exchanging energy quanta matching the energy gap between the dark states and lower polariton into vibrational modes (vibrationally assisted scattering). To understand better how the fluorescing state of a molecule that is not strongly coupled to the cavity can transfer its excitation energy to the lower polariton in the radiative pumping mechanism, we performed multi-scale molecular dynamics simulations. The results of these simulations suggest that non-adiabatic couplings between uncoupled molecules and the polaritons are the driving force for this energy transfer process.

Published under license by AIP Publishing. https://doi.org/10.1063/5.0037896

I. INTRODUCTION

Recent observations of modified chemistry in the strong light–matter coupling regime[1–8] have significantly increased the scientific interest of, in particular, chemists in this field. The strong coupling regime is achieved when the rate of energy exchange between molecules and confined light modes, such as those occurring inside Fabry–Pérot cavities or near surface plasmons, exceeds the decay rates of both the molecules and the confined light modes.[1,9,10] Under these conditions, excitations of the molecules and light modes hybridize and form new light–matter states called polaritons.[11–13] To systematically exploit polaritons for controlling chemistry, a complete understanding of the effects of strong coupling on the molecular dynamics, and in particular the relaxation of polaritons, is essential.

Polariton decay has been studied for more than two decades,[13–26] but neither the precise mechanistic details nor how to control this process is fully understood yet. The picture that emerges from both experiments and phenomenological theories suggests that polariton decay involves both vibrationally assisted scattering (VAS) and radiative pumping.[13,20,22,27–29] In VAS, transitions between the light–matter states are accompanied by changes in the vibrational eigenstates of specific modes and are manifested by an increased photoluminescence (PL) intensity when such modes are resonant with energy gaps between polaritonic states.[22] Radiative pumping involves a direct exchange of a photon between uncoupled molecules and polariton states, but the details of this mechanism are poorly understood.[13,27–29]

Experimental evidence for the radiative pumping mechanism was obtained from photoluminescence measurements on cavity

systems in which there is an emitting state that overlaps with the polariton branch. Examples of such systems include (i) single-walled carbon nanotubes with sp^3-defects that trap excitations at a lower energy,[30] (ii) BODIPY dyes that form excimers with reduced energy gaps,[29] or (iii) mixtures in which excitation of an uncoupled dye that has an absorption and emission below that of the coupled dye efficiently populates the lower polariton (LP) branch.[28]

Because organic molecules have intrinsic Stokes shifts due to different equilibrium geometries in the electronic excited state, we postulate that the contribution of radiative pumping to polaritonic decay, and hence the ratio between the two scattering channels, should depend directly on the Stokes shift.

To test our conjecture, we measured the photoluminescence (PL) of two strongly coupled cavity–molecule systems, with one cavity containing Rhodamine 6G (R6G), a dye with a Stokes shift of 27 nm (110 meV), typical for organic dyes and the other cavity containing the J-aggregate of 5,6-dichloro-2-[[5,6-dichloro-1-ethyl-3-(4-sulfobutyl)-benzimidazol-2-ylidene]-propenyl]-1-ethyl-3-(4-sulfobutyl)-benzimidazolium hydroxide sodium salt (TDBC), which has a negligible Stokes shift of only 2 nm (7 meV). The similarity between the PL spectra of the R6G cavity on the one hand and the convolution of the R6G fluorescence with the cavity transmission spectrum on the other hand suggests that radiative pumping dominates for strongly coupled molecules with large Stokes shifts. In contrast, for strongly coupled TDBC J-aggregates, which lack overlap between their emission spectra and the lower polariton (LP) branch, the dominant relaxation channel involves VAS, in particular when the Rabi splitting is large.

In addition, we also investigate the mechanism of radiative pumping in atomic detail by means of multi-scale molecular dynamics simulations.[31–33] The results of these simulations suggest that the driving force for radiative pumping is the non-adiabatic coupling between weakly coupled or uncoupled molecular states and the bright polaritons, rather than photon exchange.

II. METHODS

A. Sample fabrication

The samples were fabricated on top of 20×20 mm^2 sized pieces of 1 mm thick BK7 glass substrates that were precleaned by sonication in acetone followed by rinsing with isopropanol alcohol and drying under dry nitrogen flow.

The back-mirror of the cavity was formed by evaporating a 40 nm thick layer of silver on about two thirds of the substrate while shielding the rest of the substrate from the deposition by a mechanical mask. Silver was deposited using a custom-built electron beam evaporator equipped with an ultra-high vacuum chamber. The rate of evaporation was 0.5 Å/s, and the pressure during it was 10^{-8} mbar. The purpose of the mask was to leave space on the substrate so that during spin coating, this area on the sample will get covered with the polymer film with molecules, but no cavity will be formed due to the absence of mirrors. This area was used as reference for the uncoupled molecules.

After evaporating the first mirror, a molecule–polymer film was spin-coated on top of the substrate immediately to minimize the silver oxidation due to exposure to air. After the molecule-resist layer was hardened, the second silver mirror was evaporated on top of

it, following the same procedure as above. Finally, a thin, about 10 nm, protective layer of poly(methyl methacrylate) (PMMA) was spin-coated on top of the second mirror to prevent the silver from oxidizing.

The preparation of the molecule–polymer solution for spin-coating is the most critical step. In addition to containing the desired amount of the photo-active molecule, its viscosity determines the thickness of the film together with the spinning speed and thus the resonance of the cavity. The photo-active compounds used were J-aggregates of 5,6-dichloro-2-[[5,6-dichloro-1-ethyl-3-(4-sulfobutyl)-benzimidazol-2-ylidene]-propenyl]-1-ethyl-3-(4-sulfobutyl)-benzimidazolium hydroxide sodium salt (Few Chemicals) usually called TDBC and Rhodamine 6G (R6G, Sigma Aldrich).

For TDBC samples, the molecule–polymer solution was prepared by mixing the required amount of solid TDBC powder with Millipore water to reach the target concentration, i.e., 5 and 10 mM for the low and high concentration samples, respectively. After dissolving the TDBC molecules, poly(vinyl alcohol) (PVA) was added into the solution as solid grains to obtain a final mass concentration of 5%. PVA was dissolved by mixing the solution with a magnetic stirrer at 80 °C for 12 h. Finally, the solution was filtered with a 0.2 μm pore size filter to get rid of possible impurities and undissolved PVA. To make the final spin solution, the above solution was diluted with enough Millipore water to reach the target film thickness of close to 140 nm. After spin-coating, the samples were baked for 3 min on a hot plate at 80 °C.

To obtain molecule–polymer solution for R6G samples, first, 1.98 g of SU-8 epoxy-based negative polymer resist (Microchem SU-8 2100) was dissolved in 9.63 ml of cyclopentanone, and R6G molecule powder was dissolved in ethanol to obtain 28 mM solution. To get rid of possible molecular aggregations, the R6G solution was filtered with 0.2 μm pore size filter. Finally, the dye solution and the polymer solutions were mixed together and diluted with a suitable amount of cyclopentanone to make the spin solution for a 130 nm thick film. After spin-coating, the samples were baked for 3 min on a hot plate at 95 °C and cured with UV-light for 1 min. A schematic cross section of a typical cavity sample is shown in the inset of Fig. 1.
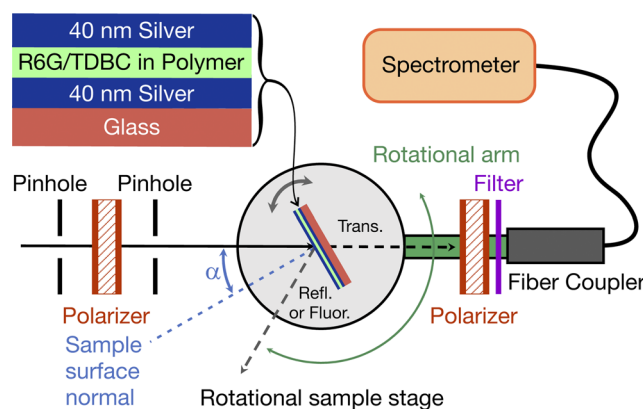

FIG. 1. Schematics of the experimental setup and the sample structure.

B. Angle-resolved steady state measurements

Angle-resolved *transmittance*, $T(\alpha) = I_{\text{Trans}}(\alpha)/I_{0,\text{Trans}}(\alpha)$, was measured in the optical frequency range using a home-built measurement setup schematically presented in Fig. 1. Here, $I_{0,\text{Trans}}(\alpha)$ is the angle-dependent intensity transmitted through a plain substrate glass. The sample was installed on a rotating stage with the cavity pointing toward the excitation light and front surface on a rotation axis. An Oriel 66182 white light source was used for excitation. The light was collimated and aligned by two pinholes with a rotatable prism polarizer in between to adjust the polarization. The incident angle of the incoming light was adjusted manually by rotating the goniometric mount. The transmitted signal was collected using a fiber coupler assembly F220SMA-A (ThorLabs) with f = 10.9 mm and NA = 0.25, which was connected to an optic fiber. Another polarizer was positioned in front of the collection assembly, and it followed the excitation polarization. The radiation was guided into a Jobin Yvon iHR320 spectrometer equipped with a Jobin Yvon Symphony CCD camera, and the spectra were collected on a computer in ASCII (American Standard Code for Information Interchange) format. In all the presented experiments, the excitation light was *S*-polarized. Experiments carried out with *P*-polarized light produced similar results (data not shown).

Photoluminescence (PL) as a function of the detection angle was collected from the cavity samples with the same home-built setup that was used for the transmittance measurements (see Fig. 1). As an excitation source, we used a continuous wave (CW) argon ion laser with a few selectable output wavelengths. *S*-polarization was chosen for the laser excitation and PL detection in all cases. The resonance condition, i.e., the minimum separation between the polariton branches where the upper polariton (UP) and LP absorption peaks have approximately equal amplitude and the coupling strength is the largest, was achieved for most of the samples at an angle of incidence of α = 30° (see Fig. 2 and Fig. S3). Thus, α = 30° was used as an excitation angle for all the cavities. This also enabled us to resonantly excite the upper polariton (UP) state with the available laser lines. For R6G, we used the 488.1 nm laser line, and for TDBC, we used the 515.4 nm laser line.
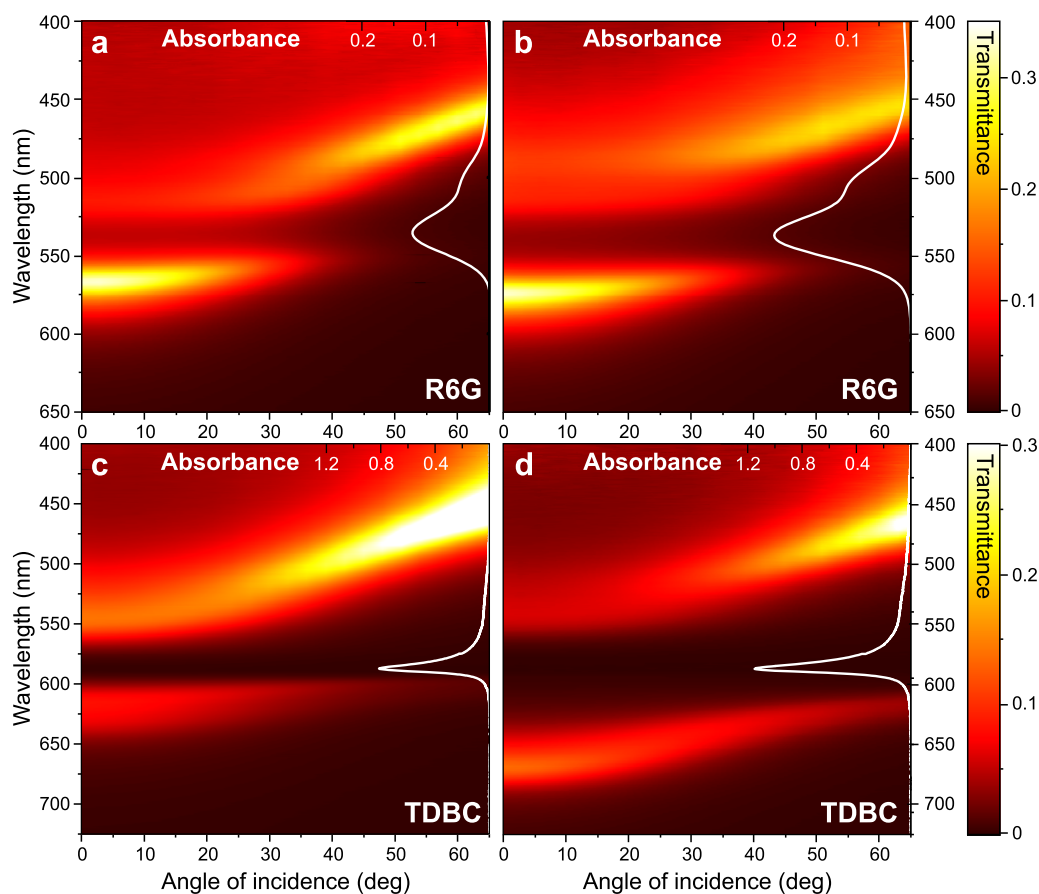

FIG. 2. Angle dependent transmittances (contour map) of cavities having (a) low and (b) high concentrations of R6G and different amounts of J-aggregates of TDBC: (c) low concentration and (d) high concentration. The absorption spectra of the bare molecular films are shown on the right axis with the absorbance scale at the top.

Because the position of the LP branch visible in our PL measurements with the laser coincides with that of the LP branch observed in the transmission and reflectivity measurements with the lamp, we infer that the laser power was sufficiently low to remain within the linear absorption regime. Thus, we avoid two-photon absorption, and the available polaritons are excited by at most one photon. Care was taken that the transmittance data and emission data were measured exactly from the same measurement point of the cavity. Dielectric filter (Semrock) was used to avoid any scattering from the excitation laser entering the fiber coupler. Steady-state *absorbance* $[-\text{Log}(T)]$ was collected from molecule–polymer films using a commercial UV/vis absorption spectrophotometer (Perkin Elmer, Lambda 850).

C. Molecular dynamics simulations

We simulated an ensemble of 64 Rhodamine molecules inside a lossy optical cavity supporting 16 modes. The lifetime of the cavity was 15 fs. The hybrid quantum mechanics/molecular mechanics (QM/MM) model proposed by Luk *et al.* was used to describe the Rhodamine molecules.[31] In brief, the fused ring system of Rhodamine was included in the QM region and modeled with RHF/3-21G in the electronic ground state and with CIS/3-21G in the electronic excited state. The rest of the fluorophore and the water molecules were modeled with the Amber03 force field.[34] The cavity

simulation was performed with Gromacs 4.5.3,[35] using the QM/MM interface to TeraChem.[36,37]

III. RESULTS AND DISCUSSION

To study the effect of the molecular Stokes shift on the polariton relaxation, we fabricated Fabry–Pérot cavities with 40 nm thick silver mirrors separated by a thin polymer film containing optically active compounds with different Stokes shifts. The selected molecular compounds were R6G, which has an absorption maximum at a wavelength of 537 nm and a Stokes shift of about 27 nm when embedded in the polymer matrix (see Fig. S1), and J-aggregates of TDBC with an absorption maximum at 587 nm and a negligible Stokes shift (~2 nm). Altogether, we fabricated four cavities having two different concentrations of each molecule embedded in their polymer layers.

Molecular concentrations within the polymer were 137 and 275 mM for R6G and 123 and 245 mM for TDBC. To accurately characterize the absorption of the molecules, we measured separately the same films without a cavity. The absorption spectra of the fabricated molecule–polymer films are shown on the right axis of the dispersion plots in Fig. 2 and with more details in the supplementary material (Fig. S1). We also fabricated an identical cavity without any photo-active molecules inside the polymer layer. The dispersion of this plain cavity is shown in the supplementary material (Fig. S2).
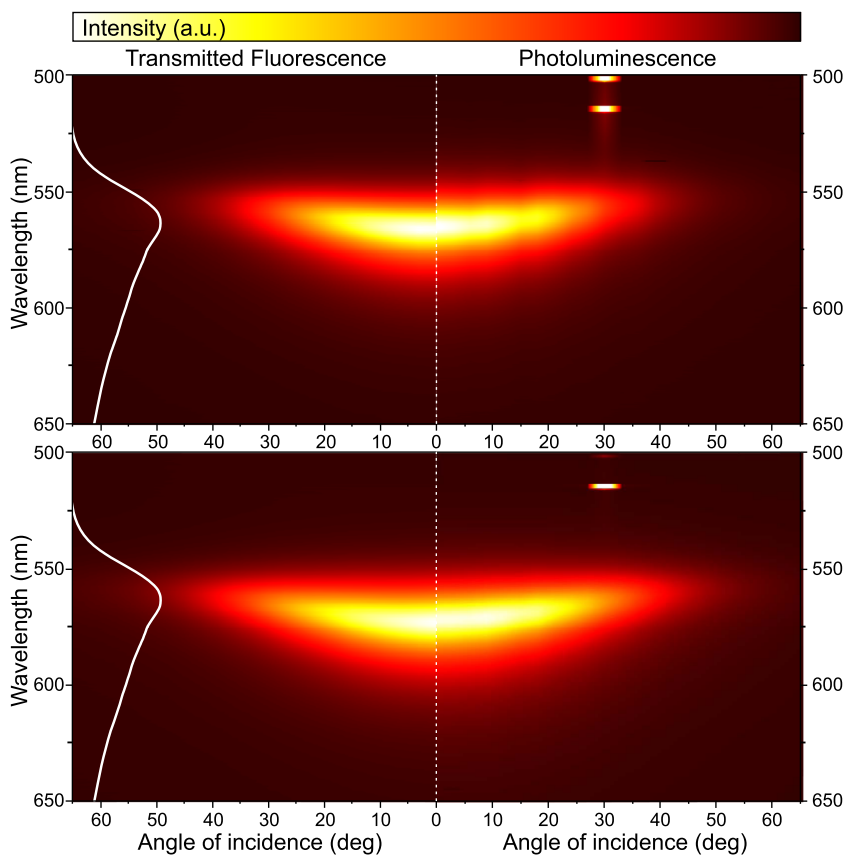
FIG. 3. Measured angle-resolved-photoluminescence of the R6G cavities with low (upper row) and high (lower row) molecular concentrations is shown in the right panels. The left panels show the product of the transmittance of the same cavity (see Fig. 2) on the one hand and the fluorescence spectrum of the R6G polymer film, which is shown separately on the left axis (white line), on the other hand. The bright spots in the right panels at 30° are artifacts caused by the excitation laser leaking onto the detector when the detection angle and excitation angle coincide.

From the transmittance spectra, we estimate the Q-factor of the cavity to vary between 14, at a 0° angle of incidence, and 20, at a 70° angle of incidence.

A. Dispersions

We measured the transmittance spectra of these cavities while varying the angle of incidence. The measured data are shown as contour plots in Fig. 2. A clear dispersion with a wide Rabi splitting or avoided crossing, at the wavelength of the molecular absorption maximum, i.e., at the molecular excitation energy, E_{Mol}, was observed for all the cavity systems, suggesting that they are all in the strong coupling regime.

We determined the widths of the Rabi splittings from the minimum separation between the upper and lower polariton (UP and LP) branches in the dispersion, which happens at the resonance angle corresponding to the resonant wavevector, k. The resonance angle was estimated as the angle where the transmittance peaks corresponding to the LP and UP have equal heights, as shown in the supplementary material (Fig. S3). The estimated Rabi energies were 210 and 365 meV for the low and high concentrations of R6G, respectively, and 255 and 506 meV for the low and high concentrations of TDBC.

In addition to the main absorption peak, the absorption spectrum of R6G also contains a higher-energy shoulder (Fig. 2 and Fig. S1). The main peak and the shoulder correspond to the 0–0 and 0–1 vibronic transitions in R6G, respectively. Because there are, thus, two electronic transitions in the energy range that we investigated, the R6G-cavities have a double Rabi splitting with three polariton states: LP, UP, and a middle polariton (MP).[25,38,39] However, the splitting between the MP and UP is rather small, and the transmittance peaks of the MP and UP are spectrally partially overlapping but still visible (see Fig. S3). As we, nevertheless, estimated the Rabi splitting as the separation between the LP and UP, we introduced a small error in our estimates. This error was manifested in a slight deviation of the square root dependence of the estimated Rabi splitting with the molecular concentration. However, because our further analysis is based on the measured dispersion curves rather than these estimates, it had no effect on the conclusions.

B. Photoemission

To analyze the relaxation pathways of the photo-excited cavities, we mapped out their angular photoluminescence (PL) under continuous excitation of UP states close to the resonance angle. See experimental methods for the exact values for all cavities. The measured PL intensities for the R6G cavities are shown on the right-hand side of Fig. 3. They closely follow the dispersion of the LP with most of the intensity concentrating at the lowest energies and angles, in good agreement with earlier findings.[12,40]

Previously,[17,20,24,32] it has been shown that the excitation of the UP leads to a very fast relaxation of the excitation energy into dark states (DS, also called the exciton reservoir) as shown schematically by narrow blue arrows in Fig. 4. These dark states consist of weakly coupled or uncoupled molecular excitations and delocalized superpositions of them with a negligible contribution of the cavity photon. Their energies are close to the energy of the molecular excitation, E_{Mol}, following the distribution of the molecular absorption as illustrated schematically in Fig. 4 by a blue distribution.[21]
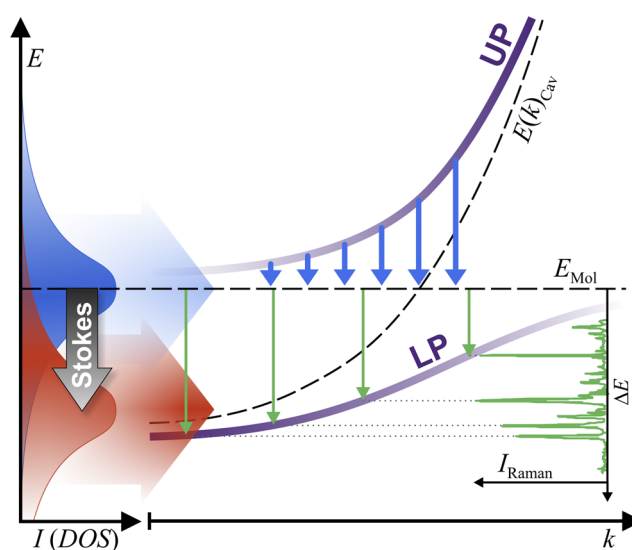

FIG. 4. Schematic presentation of the relaxation pathways after an excitation of the UP. Blue narrow arrows show the fast relaxation into the dark states represented as the blue distribution. This is followed by either relaxation into the fluorescing state (red distribution) with an energy offset determined by the Stokes shift of the molecule, and subsequent radiative pumping of the LP from there, shown as the wide red arrow, or direct vibrationally assisted scattering (VAS) into the LP directly from the dark states, shown as narrow green arrows. The green Raman spectrum shows the vibrational energies of the molecules (TDBC) in the dark states. In addition to these processes, there is relaxation within dark states and feeding of polaritons from there, as shown by a faint blue arrow. This induces a smooth background for PL from the LP.[13,32] (Illustration adapted from Refs. 13 and 22 to include the radiative pumping channel via the molecular fluorescent states. The Raman spectrum has been taken from Ref. 43.)

In previous work, we have shown that if the molecules have an excited state with an energy below that of the state that is strongly coupled to the cavity—like in BODIPY dyes that can form excimers with reduced energy gaps[29] or carbon nanotubes with sp³-defects that can trap excitations at a lower energy[30]—the excitation can rapidly localize into this lower energy state of one of the molecules.[25,31,33,41] For R6G, this state is the excited-state minimum from where fluorescence occurs. In what follows, we call this state the "fluorescing state."

Because the fluorescence spectrum of R6G, shown as a white line in Fig. 3, overlaps significantly with the LP branch (Fig. 2) in both R6G cavity systems, population transfer from the fluorescing state to the LP branch, known as radiative pumping,[27–30] should be feasible, at least energetically. To check this conjecture, we calculated the convolution between the fluorescence spectrum of a bare R6G molecule–polymer film and the transmittance of the LP branch. The similarity of the convoluted spectrum, plotted in the left panels of Fig. 3, to the measured cavity PL spectra suggests that localization of the excitation onto one of the molecules that form the polariton, followed by radiative pumping from the relaxed fluorescing state of the molecule into the LP branch, is the main deactivation channel in these R6G cavity systems (Fig. 4).

In contrast, because the fluorescing state of TDBC J-aggregates lies energetically above the LP branch in cavities containing TDBC,

there should be little to no overlap between the TDBC fluorescence spectrum (white line in Fig. 5) and the lower polariton branch identified in transmittance measurements (Fig. 2). We, therefore, expect that radiative pumping is not an efficient decay pathway for TDBC based cavities. In Fig. 5, we plot the measured cavity PL spectra for both TDBC cavity systems. The convolution between the transmission spectra of the TDBC cavity system [Figs. 2(c) and 2(d)] and the fluorescence spectrum of a bare TDBC molecule–polymer film does not match the PL spectrum, in particular for the cavity with the larger TDBC concentration, confirming our conjecture that radiative pumping from the fluorescent state into the LP branch is not the main relaxation channel for polaritons formed by TDBC aggregates. For the cavity with the lower TDBC concentration, the convoluted spectrum still roughly resembles the PL of the LP since some overlap between the fluorescence and LP exists for radiative pumping, but the discrepancy is evident in the case of the high concentration TDBC cavity system.

Instead, in TDBC cavities, the dominant relaxation process is VAS, first observed by Coles *et al.*[22] In addition to direct fluorescence through the thin cavity mirror, which is faintly visible in Fig. 5 as an angle independent luminescent feature, PL is observed predominantly near the minimum of the dispersive LP branch.[44] Following the ideas of Lidzey and co-workers who measured cavity PL under non-resonant excitation conditions, we formed a total PL spectrum

of the LP by summing up all the PL spectra measured at different detection angles for the high concentration TDBC cavity. In Fig. 6, we plotted this total PL intensity as a function of the energy gap, ΔE, separating the dark state manifold, which we assume is centered on the absorption maximum of the J-aggregates,[21] from the lower polariton branch (see also Fig. 4). As in the PL measurements with non-resonant excitation,[22] several distinct maxima are also observed in the total PL intensity if the cavity is excited resonantly into the UP. We compare this spectrum to a TDBC J-aggregate Raman spectrum with the Raman shift also plotted as a function of the energy gap in Fig. 6. The energy gaps at which the PL intensity is enhanced coincide nicely with the vibrational frequencies of the strongest Raman-active modes of the J-aggregate.[22,26] These observations suggest that the relaxation process involves a direct exchange of energy between polaritonic states and vibrations,[22,46] which is most efficient if the vibrational frequency is resonant with the energy gap between the dark state manifold and the LP branch (Fig. 4). This vibrationally assisted scattering channel dominates the relaxation process if the molecules lack a sufficiently deep energy minimum in the electronic excited state, as in TDBC.

While we cannot rule out VAS in R6G, the perfect overlap between the PL spectra on the one hand and the convolution of the molecular fluorescence spectrum and cavity transmittance spectra on the other hand suggests that VAS can only be a very minor
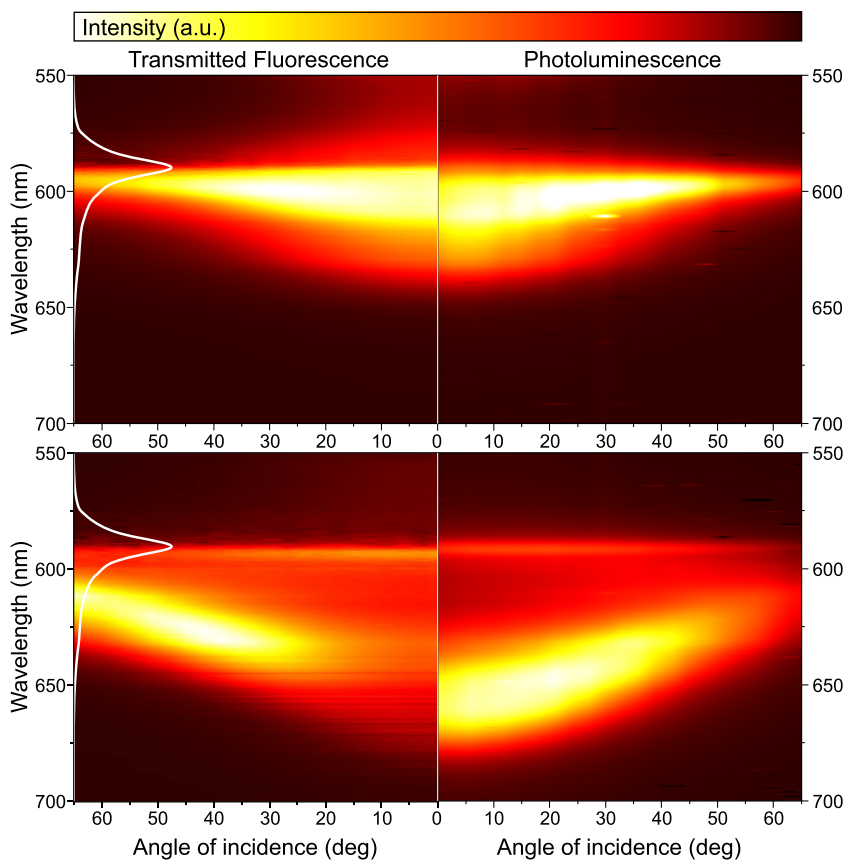

FIG. 5. Measured angle-resolved-photoluminescence of TDBC samples with low (upper row) and high (lower row) molecular concentrations is shown in the right panels. The left panels show the product of the transmittance of the sample and the fluorescence spectrum of the TDBC polymer film, which is shown separately on the left axis (white line).
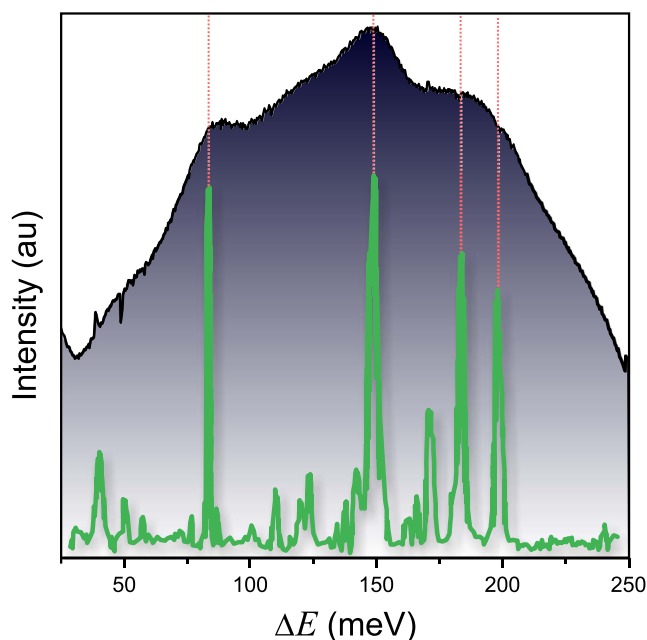
FIG. 6. The dark shaded curve represents the spectral sum of intensity-normalized PL spectra measured at different angles for the high concentration TDBC cavity system. Small peaks present in all the spectra are well emphasized in this total PL spectrum, which is plotted here as a function of the energy separation, ΔE, from the dark states at 2.11 eV (587 nm, see Fig. 4). These peaks are located exactly at the positions where the energy separation from the dark states matches with the strongest vibrational energies of TDBC J-aggregates, as demonstrated by the Raman spectrum (green) of TDBC J-aggregates. The Raman spectrum has been taken from Ref. 43.

channel for R6G. We note that in addition to the high spectral overlap between the fluorescence and LP discussed above, also the high luminescence quantum yield of R6G may contribute to the efficiency of RP. However, without the essential spectral overlap, a high emission quantum yield alone does not guarantee efficient RP. Likewise, some radiative pumping can occur also in TDBC but only at high k-vectors (angle), where the LP branch has a small overlap with the low-energy tail of the TDBC fluorescence spectrum. Because we do observe emission in this region, we infer that in TDBC, radiative pumping takes place in addition to VAS, in particular in the cavity with the lower concentration.

In addition to the scattering from the dark states into the LP by exchanging energy with discrete molecular vibrational modes, vibrationally assisted scattering involving energy exchange with the thermal bath of lower frequency modes also occurs as evidenced by the smooth background that masks the peaks at the molecular Raman frequencies in Fig. 6. These lower frequency modes are provided by, e.g., the polymer matrix, and their involvement in the polariton relaxation pathway has been investigated experimentally, theoretically, and with computer simulations.[13,20,32]

We note that in other recent studies of similar R6G cavity systems, in addition to the PL of the LP branch, a separate angle independent luminescent feature has also been detected at the wavelength of the molecular fluorescence maximum.[25,39] In our R6G

cavity systems, we only see clear emission from the LP branch without this additional feature. The reason for this is that our cavities are less detuned, and the maximum of the fluorescence spectrum still overlaps well with LP, thus providing efficient RP of the LP. In the case of larger detuning, like in Ref. 39, the intensity of the fluorescence mediated LP emission is already so small that a regular fluorescence leaking through the thin cavity mirror will be visible as a separate angle-independent emission branch at the fluorescence maximum. However, because the fluorescence maximum of TDBC is well above the LP minimum in our TDBC cavity systems, we do see this angle independent luminescence at the wavelength of the fluorescence maximum (Fig. 5), as discussed above also.

C. Molecular dynamics simulations

To understand whether the excited state minimum, i.e., the fluorescing state, provides a direct access to the LP in the radiative pumping mechanism and to gain insight into the driving force behind this mechanism, we performed MD simulations with our multi-scale Tavis–Cummings model that takes into account the molecular details of the molecules coupled to the cavity.[31] In particular, we used a very recent extension of the original method that includes multiple radiation modes[45] to model the cavity dispersion.

We modeled the dynamics of an ensemble of 64 hydrated Rhodamine molecules in an optical cavity using the same hybrid quantum mechanics/molecular mechanics (QM/MM) description for the molecules as in previous works.[31,32,45] The cavity was red-detuned such that at the zero-incidence angle, the energy of the cavity mode is 0.22 eV below the absorption maximum of our Rhodamine model (4.18 eV in our QM/MM model[32]). This detuning was chosen to match the emission maximum of our Rhodamine model at 3.99 eV.[31] The cavity dispersion was modeled by 16 discrete modes, and the cavity lifetime was set to 15 fs. Prior to the simulation of the cavity system, 63 Rhodamine molecules were equilibrated for 5 ps on the ground-state (S_0) potential energy surface, while one molecule was equilibrated on the excited-state (S_1) potential energy surface, resulting in the molecule sampling the S_1 minimum, i.e., at the fluorescing state. In these frames, the lowest energy state of the molecule–cavity system is at 3.62 eV and is localized (0.97) at the molecule equilibrated in S_1.

As shown in the population plots of Figs. 7(c) and 7(d), the molecular component rapidly reduces from 0.97 to around 0.5, while simultaneously the photonic contribution of the cavity modes rises from 0 to 0.5, indicating the formation of a hybrid light–matter polaritonic state. This polaritonic state then rapidly decays due to the finite cavity lifetime, as demonstrated by a steep rise in ground state population in Fig. 7(c).

Thus, the results from the simulations seem to suggest that if the excitation is localized on a single molecule that has relaxed into its S_1 minimum, i.e., the fluorescing state, non-adiabatic coupling can induce efficient population transfer from this initial state to the LP around zero angle. Based on this observation, we speculate that the driving force behind radiative pumping is non-adiabatic coupling between the bright polaritonic states and weakly coupled states, rather than the emission and reabsorption of a photon. Because of the low Q-factor, emission occurs
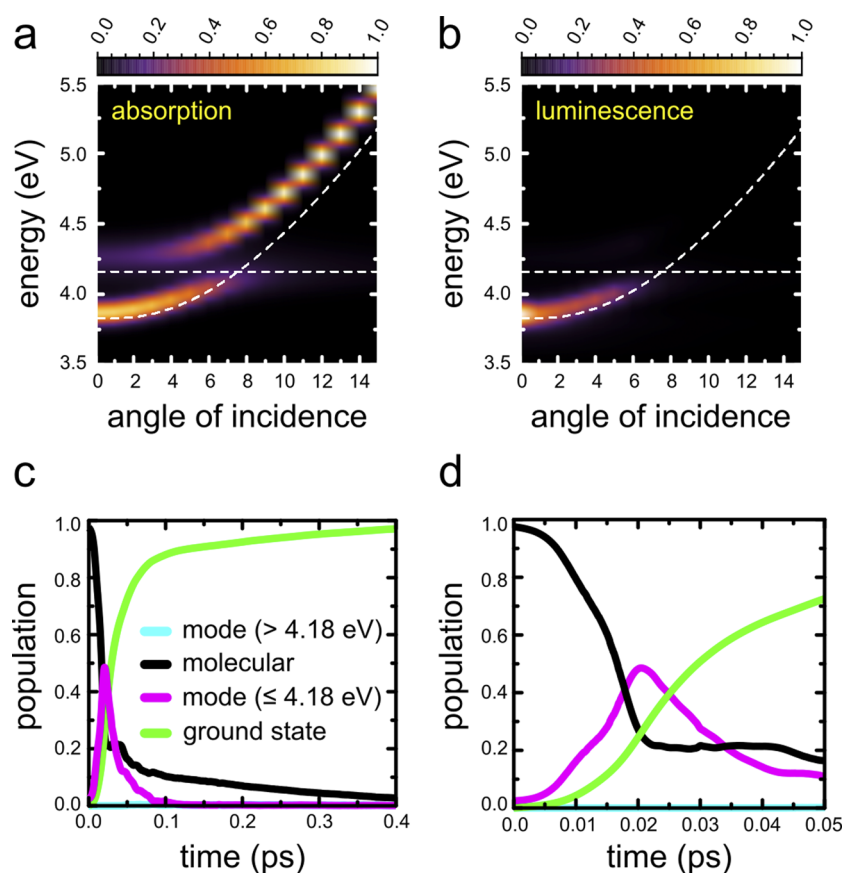
FIG. 7. Computed angle-dependent absorption (a) and photoluminescence spectrum (b) of an optical cavity with 64 Rhodamine molecules, starting from a configuration in which one of the Rhodamine molecules is in the S_1 minimum geometry. The total population of all molecular states (black), all cavity modes at energies below (magenta) and above (cyan) the molecular absorption maximum (4.18 eV), and the ground state (green) is shown in (c). Panel (d) is a zoom-in on the first 50 fs. The dashed white lines in (a) and (b) indicate the dispersion of an empty cavity and absorption maximum of Rhodamine. The incidence angles correspond to (discretized) wavevectors (see Ref. 45 for details).

from this state, as demonstrated by the angle-dependent photoluminescence spectra in Fig. 7(b). These results, therefore, support the hypothesis that the fluorescing state connects the dark state manifold to the lower polariton via the radiative pumping mechanism.

We note that in our simulations, the rate at which the population transfers from the molecular fluorescing state to the lower polariton branch exceeds the radiative pumping rates observed in time-resolved photoluminescence experiments.[23,24,42] This discrepancy is due to coupling a much smaller number of molecules (64) to the cavity in our simulations, as compared to experiments. Experimentally, strong coupling is achieved by coupling of the order of 10^5 molecules to the cavity.[48] To reach the strong coupling regime also in simulations with only 64 molecules, we had to significantly enhance the cavity vacuum field. Because the non-adiabatic coupling directly depends on the strength of the cavity vacuum field, the non-radiative population transfer rate is overestimated. Simulations with a more realistic vacuum field and hence a larger number of molecules require significant computational resources and will be presented in future work. Nevertheless, despite a much higher rate, we believe that the radiative pumping mechanism observed in our simulations provides a plausible alternative to the previously proposed mechanism that involves direct emission and re-absorption of a photon.

IV. CONCLUSIONS

Summarizing, we have shown that the Stokes shift can determine which of the two main polariton scattering channels, vibrationally assisted scattering or radiative pumping, is the dominant one. In addition, we have also investigated the mechanism of the radiative pumping in atomic detail with multi-scale molecular dynamics simulations. Based on the results of the simulation, we speculate that the driving force for radiative pumping is the non-adiabatic coupling between weakly coupled or uncoupled molecular states on the one hand and the bright polaritons on the other hand, rather than photon exchange. Our findings suggest that the molecular degrees of freedom, and in particular the Stokes shift, are important parameters to take into consideration when planning or analyzing experiments on strongly coupled molecule–cavity systems. Because the relaxation process strongly depends on the Stokes shift, polariton dynamics can be controlled via a judicious choice of molecules, which can be important for applications, such as polaritonic lasing[47] or coherent light harvesting.[33]

SUPPLEMENTARY MATERIAL

See the supplementary material for additional spectral data.

AUTHORS' CONTRIBUTIONS

E.H. and S.P. contributed equally to this work.

ACKNOWLEDGMENTS

DATA AVAILABILITY

The data that support the findings of this study are available from the corresponding author upon reasonable request.

REFERENCES

[1]R. F. Ribeiro, L. A. Martínez-Martínez, M. Du, J. Campos-Gonzalez-Angulo, and J. Yuen-Zhou, Chem. Sci. **9**, 6325–6339 (2018).

[2]J. A. Hutchison, T. Schwartz, C. Genet, E. Devaux, and T. W. Ebbesen, Angew. Chem., Int. Ed. **51**, 1592–1596 (2012).

[3]K. Stranius, M. Herzog, and K. Börjesson, Nat. Commun. **9**, 2273 (2018).

[4]A. Thomas, J. George, A. Shalabney, M. Dryzhakov, S. J. Varma, J. Moran, T. Chervy, X. Zhong, E. Devaux, C. Genet, J. A. Hutchison, and T. W. Ebbesen, Angew. Chem., Int. Ed. **55**, 11462–11466 (2016).

[5]J. Lather, P. Bhatt, A. Thomas, T. W. Ebbesen, and J. George, Angew. Chem., Int. Ed. **58**, 10635 (2019).

[6]R. M. A. Vergauwe, A. Thomas, K. Nagarajan, A. Shalabney, J. George, T. Chervy, M. Seidel, E. Devaux, V. Torbeev, and T. W. Ebbesen, Angew. Chem., Int. Ed. **58**, 15324–15328 (2019).

[7]D. Polak, R. Jayaprakash, T. P. Lyons, L. Á. Martínez-Martínez, A. Leventis, K. J. Fallon, H. Coulthard, D. G. Bossanyi, K. Georgiou, A. J. Petty II, J. Anthony, H. Bronstein, J. Yuen-Zhou, A. I. Tartakovskii, J. Clark, and A. J. Musser, Chem. Sci. **11**, 343 (2020).

[8]B. Munkhbat, M. Wersäll, D. G. Baranov, T. J. Antosiewicz, and T. Shegai, Sci. Adv. **4**, eaas9552 (2018).

[9]V. Savona, L. C. Andreani, P. Schwendimann, and A. Quattropani, Solid State Commun. **93**, 733–739 (1995).

[10]P. Törmä and W. L. Barnes, Rep. Prog. Phys. **78**, 013901 (2015).

[11]D. G. Lidzey, D. D. C. Bradley, M. S. Skolnick, T. Virgili, S. Walker, and D. M. Whittaker, Nature **395**, 53–55 (1998).

[12]D. G. Lidzey, D. D. C. Bradley, T. Virgili, A. Armitage, M. S. Skolnick, and S. Walker, Phys. Rev. Lett. **82**, 3316–3319 (1999).

[13]D. G. Lidzey and D. M. Coles, "Strong coupling in organic and hybrid-semiconductor microcavity structures," in *Organic and Hybrid Photonic Crystals*, edited by D. Comoretto (Springer, 2015).

[14]V. Agranovich, H. Benisty, and C. Weisbuch, Solid State Commun. **102**, 631–636 (1997).

[15]D. G. Lidzey, A. M. Fox, M. D. Rahn, M. S. Skolnick, V. M. Agranovich, and S. Walker, Phys. Rev. B **65**, 195312 (2002).

[16]M. Müller, J. Bleuse, and R. André, Phys. Rev. B **62**, 16886–16892 (2000).

[17]V. M. Agranovich, M. Litinskaia, and D. G. Lidzey, Phys. Rev. B **67**, 085311 (2003).

[18]V. M. Agranovich and G. C. La Rocca, Solid State Commun. **135**, 544–553 (2005).

[19]M. Litinskaya, Phys. Lett. A **372**, 3898–3903 (2008).

[20]M. Litinskaya, P. Reineker, and V. M. Agranovich, J. Lumin. **110**, 364–372 (2004).

[21]D. M. Coles, P. Michetti, C. Clark, A. M. Adawi, and D. G. Lidzey, Phys. Rev. B **84**, 205214 (2011).

[22]D. M. Coles, P. Michetti, C. Clark, W. C. Tsoi, A. M. Adawi, J.-S. Kim, and D. G. Lidzey, Adv. Funct. Mater. **21**, 3691–3696 (2011).

[23]T. Schwartz, J. A. Hutchison, J. Léonard, C. Genet, S. Haacke, and T. W. Ebbesen, ChemPhysChem **14**, 125 (2013).

[24]T. Virgili, D. Coles, A. M. Adawi, C. Clark, P. Michetti, S. K. Rajendran, D. Brida, D. Polli, G. Cerullo, and D. G. Lidzey, Phys. Rev. B **83**, 245309 (2011).

[25]S. Baieva, O. Hakamaa, G. Groenhof, T. T. Heikkilä, and J. J. Toppari, ACS Photonics **4**, 28 (2017).

[26]N. Somaschi, L. Mouchliadis, D. Coles, I. E. Perakis, D. G. Lidzey, P. G. Lagoudakis, and P. G. Savvidis, Appl. Phys. Lett. **99**, 143303 (2011).

[27]G. H. Lodden and R. J. Holmes, Phys. Rev. B **82**, 125317 (2010).

[28]G. M. Akselrod, E. R. Young, M. S. Bradley, and V. Bulović, Opt. Express **21**, 12122 (2013).

[29]R. T. Grant, P. Michetti, A. J. Musser, P. Gregoire, T. Virgili, E. Vella, M. Cavazzini, K. Georgiou, F. Galeotti, C. Clark, J. Clark, C. Silva, and D. G. Lidzey, Adv. Opt. Mater **4**, 1615–1623 (2016).

[30]J. M. Lüttgens, F. J. Berger, and J. Zaumseil, ACS Photonics **8**, 182–193 (2020).

[31]H. L. Luk, J. Feist, J. J. Toppari, and G. Groenhof, J. Chem. Theory Comput. **13**, 4324–4335 (2017).

[32]G. Groenhof, C. Climent, J. Feist, D. Morozov, and J. J. Toppari, J. Chem. Phys. Lett. **10**, 5476–5483 (2019).

[33]G. Groenhof and J. J. Toppari, J. Phys. Chem. Lett. **9**, 4848 (2018).

[34]Y. Duan, C. Wu, S. Chowdhury, M. C. Lee, G. Xiong, W. Zhang, R. Yang, P. Cieplak, R. Luo, T. Lee, J. Caldwell, J. Wang, and P. Kollman, J. Comput. Chem. **24**, 1999–2012 (2003).

[35]B. Hess, C. Kutzner, D. van der Spoel, and E. Lindahl, J. Chem. Theory Comput. **4**, 435–447 (2008).

[36]I. S. Ufimtsev and T. J. Martinez, J. Chem. Theory Comput. **5**, 2619–2628 (2009).

[37]A. V. Titov, I. S. Ufimtsev, N. Luehr, and T. J. Martinez, J. Chem. Theory Comput. **9**, 213–221 (2013).

[38]T. K. Hakala, J. J. Toppari, A. Kuzyk, M. Pettersson, H. Tikkanen, H. Kunttu, and P. Törmä, Phys. Rev. Lett. **103**, 053602 (2009).

[39]M. O. Faruk, N. Jerop, and M. A. Noginov, J. Opt. Soc. Am. B **37**, 3200 (2020).

[40]A. Genco, A. Ridolfo, S. Savasta, S. Patanè, G. Gigli, and M. Mazzeo, Adv. Opt. Mater. **6**, 1800362 (2018).

[41]M. A. Koponen, U. Hohenester, T. K. Hakala, and J. J. Toppari, Phys. Rev. B **88**, 085425 (2013).

[42]J. George *et al.*, Faraday Discuss. **178**, 281 (2015).

[43]D. M. Coles, A. J. H. M. Meijer, W. C. Tsoi, M. D. B. Charlton, J.-S. Kim, and D. G. Lidzey, J. Phys. Chem. A **114**, 11920–11927 (2010).

[44]P. A. Hobson, W. L. Barnes, D. G. Lidzey, G. A. Gehring, D. M. Whittaker, M. S. Skolnick, and S. Walker, Appl. Phys. Lett. **81**, 3519–3521 (2002).

[45]R. H. Tichauer, J. Feist, and G. Groenhof, J. Chem. Phys. **154**, 104112 (2021).

[46]A. I. Tartakovskii, M. Emam-Ismail, D. G. Lidzey, M. S. Skolnick, D. D. C. Bradley, S. Walker, and V. M. Agranovich, Phys. Rev. B **63**, 121302 (2001).

[47]S. Kéna-Cohen and S. R. Forrest, Nat. Photonics **4**, 371–375 (2010).

[48]T. W. Ebbesen, Acc. Chem. Res. **49**, 2403–2412 (2016).